

Mass effects in the polarized virtual photon structure ^{*}

Ken Sasaki^a and Tsuneo Uematsu^b

^aDepartment of Physics, Faculty of Engineering, Yokohama National University, Yokohama 240-8501, Japan

^bDepartment of Physics, Graduate School of Science, Kyoto University, Kyoto 606-8501, Japan

We discuss target mass effects in the polarized virtual photon structure functions $g_1^\gamma(x, Q^2, P^2)$, $g_2^\gamma(x, Q^2, P^2)$ for the kinematic region $\Lambda^2 \ll P^2 \ll Q^2$, where $-Q^2(-P^2)$ is the mass squared of the probe (target) photon. We obtain the expressions for the structure functions in closed form by inverting the Nachtmann moments for the twist-2 and twist-3 operators. Numerical analysis shows that target mass effects appear at large x and become sizable near the maximal value of x , as the ratio P^2/Q^2 increases. Target mass effects for the sum rules of g_1^γ and g_2^γ are also discussed.

1. INTRODUCTION

We would like to talk about the virtual photon structure, especially on the mass effects in the polarized photon structure functions. In the last several years, there has been much interest in the spin-dependent photon structure functions which can be studied in the polarized version of the ep collider or more directly in the polarized e^+e^- collision in the future linear collider (Figure.1).

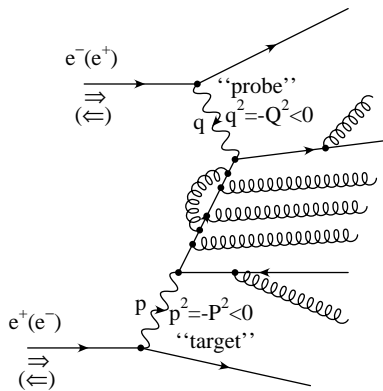


Figure 1. Two-photon process in polarized e^+e^- collision

Now let us consider the two-photon process in the polarized electron-positron collision where

^{*}Talk presented by T. Uematsu at Loops and Legs 2004, Zinnowitz, Germany, April 25-30, 2004. YNU-HEPTh-04-101; KUNS-1922.

both of the photons are off-shell. We particularly consider the case where the mass square of the “probe” photon, Q^2 , is much bigger than that of the “target” photon, P^2 , which is in turn much bigger than the square of the QCD scale, Λ^2 . The advantage for studying the virtual photon target in this kinematical region is that we can calculate whole structure functions g_1^γ and g_2^γ in perturbative QCD up to next-leading-order (NLO), in contrast to the real photon target where there remain uncalculable non-perturbative pieces. Note that the 1st moment of g_1^γ is related to the axial anomaly just like the nucleon case, while the second structure function g_2^γ only exists for the virtual photon target ($P^2 \neq 0$).

Now the possible mass effects are twofold; target-mass effects and quark-mass effects. Here in this talk we discuss the former, which appear as power-corrections in P^2/Q^2 . For the real photon target ($P^2 = 0$), there is no need to consider target mass corrections. But when the target becomes off-shell and for relatively low values of Q^2 , contributions suppressed by powers of $\frac{P^2}{Q^2}$ may become important. Then we need to take into account these target mass contributions just like the case of the nucleon structure functions. The consideration of target mass effects (TME) is important by another reason. For the virtual photon target, the maximal value of the Bjorken

variable x is not 1 but

$$x_{\max} = \frac{1}{1 + \frac{P^2}{Q^2}}, \quad (1)$$

due to the constraint $(p+q)^2 \geq 0$, which is contrasted with the nucleon case where $x_{\max} = 1$. The structure functions should vanish at $x = x_{\max}$. However, the NLO QCD result [1] for $g_1^\gamma(x, Q^2, P^2)$ (See also the second paper of [2]) shows that the predicted graph does not vanish but remains finite at $x = x_{\max}$. In this talk we discuss the TME for $g_1^\gamma(x, Q^2, P^2)$ and $g_2^\gamma(x, Q^2, P^2)$ in the framework of operator product expansion (OPE) supplemented by the renormalization group (RG) method [3].

2. STRUCTURE FUNCTIONS

Let us consider the structure tensor $W_{\mu\nu\rho\tau}(p, q)$ which is the absorptive part of the forward scattering amplitude $T_{\mu\nu\rho\tau}(p, q)$ (Figure 2):

$$W_{\mu\nu\rho\tau}(p, q) = \frac{1}{\pi} \text{Im} T_{\mu\nu\rho\tau}(p, q). \quad (2)$$

for the target photon with mass squared $p^2 = -P^2$ probed by the photon with $q^2 = -Q^2$.

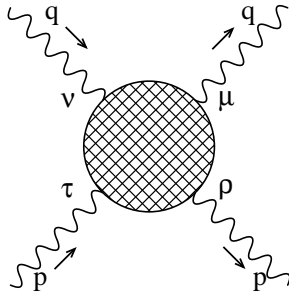


Figure 2. Virtual photon-photon scattering

The antisymmetric part $W_{\mu\nu\rho\tau}^A$ under $\mu \leftrightarrow \nu$ and $\rho \leftrightarrow \tau$, can be decomposed as

$$W_{\mu\nu\rho\tau}^A = \epsilon_{\mu\nu\lambda\sigma} q^\lambda \epsilon_{\rho\tau}^{\sigma\beta} p_\beta \frac{1}{p \cdot q} g_1^\gamma + \epsilon_{\mu\nu\lambda\sigma} q^\lambda (p \cdot q \epsilon_{\rho\tau}^{\sigma\beta} p_\beta - \epsilon_{\rho\tau\alpha\beta} p^\beta p^\sigma q^\alpha) \frac{1}{(p \cdot q)^2} g_2^\gamma \quad (3)$$

which gives two spin-dependent structure functions, $g_1^\gamma(x, Q^2, P^2)$ and $g_2^\gamma(x, Q^2, P^2)$. When the

target is real photon ($P^2 = 0$), g_2^γ is identically zero, and there exists only one spin structure function, $g_1^\gamma(x, Q^2)$. While, for the off-shell or virtual photon ($P^2 \neq 0$) target, we have two spin-dependent structure functions g_1^γ and g_2^γ .

The deep inelastic photon-photon scattering (Figure 2.) amplitude relevant for the polarized structure functions is given by

$$T_{\mu\nu\rho\tau}^A = i \int d^4x e^{iq \cdot x} \times \langle 0 | T(A_\rho(-p)(J_\mu(x)J_\nu(0))^A A_\tau(p)) | 0 \rangle_{\text{Amp}}. \quad (4)$$

For the product of the two electromagnetic currents we apply the OPE and obtain for the μ - ν antisymmetric part

$$i \int d^4x e^{iq \cdot x} T(J_\mu(x)J_\nu(0))^A = -i \epsilon_{\mu\nu\lambda\sigma} q^\lambda \sum_{n=1,3,\dots} \left(\frac{2}{Q^2}\right)^n q_{\mu_1} \cdots q_{\mu_{n-1}} \times \left\{ \sum_i E_{(2)i}^n R_{(2)i}^{\sigma\mu_1 \cdots \mu_{n-1}} + \sum_i E_{(3)i}^n R_{(3)i}^{\sigma\mu_1 \cdots \mu_{n-1}} \right\} \quad (5)$$

where $R_{(2)i}^n$ and $R_{(3)i}^n$ are the twist-2 and twist-3 operators, respectively, and are both traceless, and $E_{(2)i}^n$ and $E_{(3)i}^n$ are corresponding coefficient functions. The twist-2 operators $R_{(2)i}^n$ have totally symmetric Lorentz indices $\sigma\mu_1 \cdots \mu_{n-1}$, while the indices of twist-3 operators $R_{(3)i}^n$ are totally symmetric among $\mu_1 \cdots \mu_{n-1}$ but antisymmetric under $\sigma \leftrightarrow \mu_i$.

For the photon target we evaluate “matrix elements” of the traceless operators $R_{(2)i}^n$ and $R_{(3)i}^n$ sandwiched by two photon states with momentum p , which are written in the following forms:

$$\langle 0 | T(A_\rho(-p) R_{(2)i}^{\sigma\mu_1 \cdots \mu_{n-1}} A_\tau(p)) | 0 \rangle_{\text{Amp}} = -i a_{(2)i}^{\gamma,n} M_{(2)\rho\tau}^{\sigma\mu_1 \cdots \mu_{n-1}}, \quad (6)$$

$$\langle 0 | T(A_\rho(-p) R_{(3)i}^{\sigma\mu_1 \cdots \mu_{n-1}} A_\tau(p)) | 0 \rangle_{\text{Amp}} = -i a_{(3)i}^{\gamma,n} M_{(3)\rho\tau}^{[\sigma, \{\mu_1\} \cdots \mu_{n-1}]}, \quad (7)$$

where the subscript ‘Amp’ stands for the amputation of external photon lines, $a_{(2)i}^{\gamma,n}$ and $a_{(3)i}^{\gamma,n}$ are reduced photon matrix elements. The traceless ten-

sors $M_{(2)\rho\tau}^{\sigma\mu_1\cdots\mu_{n-1}}$ and $M_{(3)\rho\tau}^{[\sigma,\{\mu_1\}\cdots\mu_{n-1}]}$ satisfy the traceless conditions for $k = 2, 3$:

$$g_{\sigma\mu_i} M_{(k)\rho\tau}^{\sigma\mu_1\cdots\mu_{n-1}} = 0, \quad g_{\mu_i\mu_j} M_{(k)\rho\tau}^{\sigma\mu_1\cdots\mu_{n-1}} = 0. \quad (8)$$

Taking the “*matrix elements*” of (5) with the virtual photon states, we obtain the deep-inelastic photon-photon forward scattering amplitude.

The basic idea for treating target mass corrections exactly is to take account of trace terms in the traceless tensors properly [4,5]. We evaluate the contraction between $q_{\mu_1} \cdots q_{\mu_{n-1}}$ and the traceless tensors without neglecting any of the trace terms. The results are expressed in terms of Gegenbauer polynomials.

3. NACHTMANN MOMENTS

Now we follow the same procedures as were taken by Wandzura [6] and in Ref. [7] for the polarized nucleon case, and we obtain the analytic expression of the Nachtmann moments [4] for the twist-2 and twist-3 operators with definite spin n . By writing down the dispersion relations for the amplitudes and with the use of orthogonality relations as well as an integration formula for Gegenbauer polynomials $C_n^{(\nu)}(\eta)$, we project out $\sum_i a_{(2)i}^{\gamma,n} E_{(2)i}^n$ and $\sum_i a_{(3)i}^{\gamma,n} E_{(3)i}^n$ with definite spin n , which still include the infinite series in powers of P^2/Q^2 . We then sum up those infinite series and express them in compact analytic forms [7]. Then we obtain the Nachtmann moments [3]:

$$\begin{aligned} M_2^n &\equiv \sum_i a_{(2)i}^{\gamma,n} E_{(2)i}^n(Q^2, P^2, g) \\ &= \int_0^{x_{\max}} \frac{dx}{x^2} \xi^{n+1} \left[\left\{ \frac{x}{\xi} + \frac{n^2}{(n+2)^2} \frac{P^2 x \xi}{Q^2} \right\} \right. \\ &\quad \left. \times g_1^\gamma(x, Q^2, P^2) + \frac{4n}{n+2} \frac{P^2 x^2}{Q^2} g_2^\gamma(x, Q^2, P^2) \right] \\ &\quad (n = 1, 3, \dots), \end{aligned} \quad (9)$$

$$\begin{aligned} M_3^n &\equiv \sum_i a_{(3)i}^{\gamma,n} E_{(3)i}^n(Q^2, P^2, g) \\ &= \int_0^{x_{\max}} \frac{dx}{x^2} \xi^{n+1} \left[\frac{x}{\xi} g_1^\gamma(x, Q^2, P^2) \right. \\ &\quad \left. + \left\{ \frac{n}{n-1} \frac{x^2}{\xi^2} + \frac{n}{n+1} \frac{P^2 x^2}{Q^2} \right\} g_2^\gamma(x, Q^2, P^2) \right] \\ &\quad (n = 3, 5, \dots), \end{aligned} \quad (10)$$

where $x = Q^2/(2p \cdot q)$ and ξ , the so-called ξ -scaling variable [8], is given by

$$\xi = \frac{2x}{1 + \sqrt{1 - \frac{4P^2 x^2}{Q^2}}}. \quad (11)$$

The allowed range of ξ is $0 \leq \xi \leq 1$, and $\xi(x_{\max}) = 1$. In the nucleon case, the constraint $(p+q)^2 \geq M^2$ gives $x_{\max} = 1$ and $\xi(x=1) < 1$, leading to the problem of non-vanishing structure function at $x = 1$. The resolution to this problem was argued in refs. [8,11,15], by considering the dynamical higher-twist effects. M_2^n and M_3^n are perturbatively calculable. In fact, the perturbative QCD calculation of M_2^n has been done in LO [9] and in NLO [1,2], while the QCD analysis of M_3^n has been carried out in LO for the flavor non-singlet part in the limit of large N_c [10].

Once the moments M_2^n and M_3^n are known, we can derive $g_1^\gamma(x, Q^2, P^2)$ and $g_2^\gamma(x, Q^2, P^2)$ as functions of x by inverting M_2^n and M_3^n as follows:

$$\begin{aligned} g_1^\gamma(x, Q^2, P^2) &= 4\kappa\xi^2 \frac{(1 + \kappa\xi^2)^3}{(1 - \kappa\xi^2)^5} \left\{ 1 + \frac{2\kappa\xi^2}{(1 + \kappa\xi^2)^2} \right\} H_a(\xi) \\ &\quad - 4\kappa\xi^2 \frac{(1 + \kappa\xi^2)^2}{(1 - \kappa\xi^2)^4} \left\{ 1 + \frac{1}{1 + \kappa\xi^2} \right\} G_a(\xi) \\ &\quad + \xi \frac{(1 + \kappa\xi^2)^2}{(1 - \kappa\xi^2)^3} F_a(\xi) \\ &\quad - 8\kappa\xi^2 \frac{(1 + \kappa\xi^2)^3}{(1 - \kappa\xi^2)^5} \left\{ 1 + \frac{2\kappa\xi^2}{(1 + \kappa\xi^2)^2} \right\} H_d(\xi) \\ &\quad + 12\kappa\xi^2 \frac{(1 + \kappa\xi^2)^2}{(1 - \kappa\xi^2)^4} G_d(\xi) - 4\kappa\xi^3 \frac{1 + \kappa\xi^2}{(1 - \kappa\xi^2)^3} F_d(\xi) \end{aligned} \quad (12)$$

$$\begin{aligned} g_2^\gamma(x, Q^2, P^2) &= -6\kappa\xi^2 \frac{(1 + \kappa\xi^2)^3}{(1 - \kappa\xi^2)^5} H_a(\xi) \\ &\quad + \frac{(1 + \kappa\xi^2)^3}{(1 - \kappa\xi^2)^4} \left\{ 1 + \frac{4\kappa\xi^2}{1 + \kappa\xi^2} \right\} G_a(\xi) \\ &\quad - \xi \frac{(1 + \kappa\xi^2)^2}{(1 - \kappa\xi^2)^3} F_a(\xi) + 12\kappa\xi^2 \frac{(1 + \kappa\xi^2)^3}{(1 - \kappa\xi^2)^5} H_d(\xi) \\ &\quad - \frac{(1 + \kappa\xi^2)^4}{(1 - \kappa\xi^2)^4} \left\{ 1 + \frac{8\kappa\xi^2}{(1 + \kappa\xi^2)^2} \right\} G_d(\xi) \\ &\quad + \xi \frac{(1 + \kappa\xi^2)^3}{(1 - \kappa\xi^2)^3} F_d(\xi). \end{aligned} \quad (13)$$

where $\kappa = P^2/Q^2$ and we have introduced the following functions first discussed in ref. [11]:

$$\begin{aligned} H_{a,d}(\xi) &= \frac{1}{2\pi i} \int_{c-i\infty}^{c+i\infty} dn \xi^{-n} \frac{M_{2,3}^n}{n^2}, \\ G_{a,d}(\xi) &= \frac{1}{2\pi i} \int_{c-i\infty}^{c+i\infty} dn \xi^{-n} \frac{M_{2,3}^n}{n}, \\ \xi F_{a,d}(\xi) &= \frac{1}{2\pi i} \int_{c-i\infty}^{c+i\infty} dn \xi^{-n} M_{2,3}^n. \end{aligned} \quad (14)$$

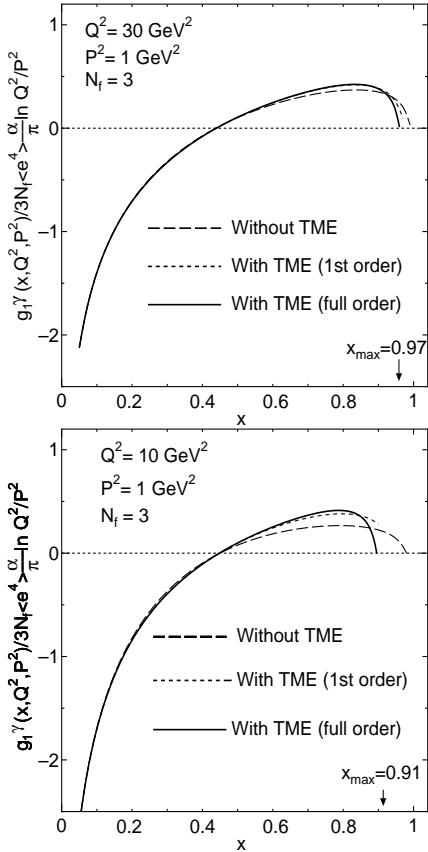


Figure 3. $g_1^\gamma(x, Q^2, P^2)$ with full TME (solid curve), with the first order TME (short-dashed curve) and without TME (dashed curve), for $Q^2 = 30$ and 10 GeV^2 with $P^2 = 1 \text{ GeV}^2$.

In Figure 3, we have shown $g_1^\gamma(x, Q^2, P^2)$ with TME as a function of x (solid curve) for $Q^2 = 30 \text{ GeV}^2$ (upper) with $P^2 = 1 \text{ GeV}^2$ and for $Q^2 = 10 \text{ GeV}^2$ (lower) with $P^2 = 1 \text{ GeV}^2$. The vertical axis is in units of $3N_f \langle e^4 \rangle / \pi \ln(Q^2/P^2)$, where $\alpha = e^2/4\pi$, the QED coupling constant, N_f is the number of active flavors, and $\langle e^4 \rangle = \sum_{i=1}^{N_f} e_i^4 / N_f$ with e_i being the electric charge of i th flavor quark. Also plotted are $g_1^\gamma(x, Q^2, P^2)$ without TME (dashed curve) and the one with TME included up to the first order in P^2/Q^2 (short-dashed curve). We observe that the target mass effects appear between intermediate x and x_{\max} , and that the effects become sizable when the ratio P^2/Q^2 is increased. The distinction between the behaviors of g_1^γ with and without TME is remarkable near x_{\max} . We get $x_{\max} \approx 0.97$ for $Q^2 = 30 \text{ GeV}^2$ with $P^2 = 1 \text{ GeV}^2$ and $x_{\max} \approx 0.91$ for $Q^2 = 10 \text{ GeV}^2$ with $P^2 = 1 \text{ GeV}^2$. The graphs of g_1^γ with TME vanish at x_{\max} as they should.

4. QCD SUM RULES WITH TME

If TME is not taken into account, the polarized virtual photon structure function $g_1^\gamma(x, Q^2, P^2)$ satisfies the following sum rule [12,1]:

$$\Gamma_1^\gamma \equiv \int_0^1 dx g_1^\gamma(x, Q^2, P^2) = -\frac{3\alpha}{\pi} \sum_{i=1}^{N_f} e_i^4 + \mathcal{O}(\alpha_s). \quad (15)$$

Note for the real photon target we have the vanishing sum rule [13]. The right-hand side corresponds to the twist-2 contribution, and actually the first term is the consequence of the QED axial anomaly. Now it will be interesting to see how this is modified when TME is included.

Once the target mass corrections are taken into account, the above sum rule is modified to the first Nachtmann moment, which reads

$$\begin{aligned} & \frac{1}{9} \int_0^{x_{\max}} dx \frac{\xi^2}{x^2} \left[5 + 4\sqrt{1 - \frac{4P^2 x^2}{Q^2}} \right] g_1^\gamma(x, Q^2, P^2) \\ & + \frac{4}{3} \int_0^{x_{\max}} dx \frac{\xi^2}{x^2} \frac{P^2 x^2}{Q^2} g_2^\gamma(x, Q^2, P^2) \\ & = -\frac{3\alpha}{\pi} \sum_{i=1}^{N_f} e_i^4 + \mathcal{O}(\alpha_s). \end{aligned} \quad (16)$$

The 1st moment of g_1^γ with TME for the nucleon target was discussed in refs. [7,14]. The power-series expansion in P^2/Q^2 gives the first order TME, the difference of LHS's of (16) and (15):

$$\Delta\Gamma_1^\gamma = - \left\{ \frac{2}{9} M_2^{n=3} + \frac{8}{9} M_3^{n=3} \right\} \frac{P^2}{Q^2} + \mathcal{O}((P^2/Q^2)^2). \quad (17)$$

The 1st moment for g_2^γ without TME known as the Burkhardt-Cottingham sum rule [16]:

$$\int_0^1 dx g_2^\gamma(x, Q^2, P^2) = 0 \quad (18)$$

turns into the one with TME given by

$$\int_0^{x_{\max}} dx g_2^\gamma(x, Q^2, P^2) = 0, \quad (19)$$

where the upper-limit of the integration has changed from 1 to x_{\max} .

5. CONCLUSION

To summarize we have studied the target mass effects in the virtual photon's spin structure functions, $g_1^\gamma(x, Q^2, P^2)$ and $g_2^\gamma(x, Q^2, P^2)$, which can be measured in the future experiments of the polarized version of the ep or e^+e^- colliders. The evaluation of kinematical target mass effects is considered to be important to extract dynamical higher-twist effects.

We have derived the expressions for $g_1^\gamma(x, Q^2, P^2)$ and $g_2^\gamma(x, Q^2, P^2)$ in closed form by inverting the Nachtmann moments for the twist-2 and twist-3 operators. Our numerical analysis shows that the target mass effects appear at large x and become sizable near $x_{\max}(= 1/(1 + \frac{P^2}{Q^2}))$, as the ratio P^2/Q^2 increases.

Here we have also examined the target mass effects for the first-moment sum rules of g_1^γ and g_2^γ . For the kinematic region we consider, the corrections to the first moment of g_1^γ turn out to be negligibly small. The first moment of g_2^γ leads to the Burkhardt-Cottingham sum rule, where only change exists in the upper limit of integration from 1 to x_{\max} .

There still remain two important subjects to be studied. The first one is the quark-mass effects

in g_1^γ and g_2^γ . The heavy flavor contribution to $g_2(x, Q^2)$ for the nucleon has been explored in ref.[17]. It would be intriguing to investigate the polarized photon case. Another subject yet to be studied is the transition from real to virtual photon, especially the 1st moment sum rule; how to reconcile the vanishing sum for the former with the non-vanishing one for the latter.

REFERENCES

1. K. Sasaki and T. Uematsu, Phys. Rev. **D59** 114011 (1999); Phys. Lett. **B473** (2000) 309; Eur. Phys. J. **C20** (2001) 283.
2. M. Glück, E. Reya and C. Sieg, Phys. Lett. **B503**, 285 (2001); Eur. Phys. J. **C20**, 271 (2001).
3. H. Baba, K. Sasaki and T. Uematsu, Phys. Rev. **D68** (2003) 054025.
4. O. Nachtmann, Nucl. Phys. **B63** (1973) 237; **B78** (1974) 455.
5. H. Georgi and H. Politzer, Phys. Rev. **D14** (1976) 1829.
6. S. Wandzura, Nucl. Phys. **B122** (1977) 412.
7. S. Matsuda and T. Uematsu, Nucl. Phys. **B168** (1980) 181.
8. A. De Rujula, H. Georgi and H. Politzer, Ann. of Phys. **103** (1977) 315; Phys. Rev. **D15** (1977) 2495.
9. K. Sasaki, Phys. Rev. **D22** (1980) 2143; Prog. Theor. Phys. Suppl. **77** (1983) 197.
10. H. Baba, K. Sasaki and T. Uematsu, Phys. Rev. **D65** (2002) 114018.
11. A. Piccione and G. Ridolfi, Nucl. Phys. **B513** (1998) 301.
12. S. Narison, G. M. Shore and G. Veneziano, Nucl. Phys. **B391** (1993) 69.
13. S. D. Bass, S. J. Brodsky and I. Schmidt, Phys. Lett. **B437** (1998) 417.
14. H. Kawamura and T. Uematsu, Phys. Lett. **B343** (1995) 346.
15. J. Blümlein and A. Tkabladze, Nucl. Phys. **B553** (1999) 427.
16. H. Burkhardt and W. N. Cottingham, Ann. of Phys. **56** (1970) 453.
17. J. Blümlein, V. Ravindran and W. L. van Neerven, Phys. Rev. **D68** (2003) 114004.